

# Susceptibility Crossover Behavior in $^3\text{He}$ and Xe Near Their Liquid-Vapor Critical Point - A Progress Report\*

Horst Meyer

*Department of Physics, Duke University, Durham, NC 27708-0305*

A discussion is presented on the crossover of the susceptibility from mean-field to Ising critical behavior upon approaching the critical point from below and from above  $T_c$ , both for  $^3\text{He}$  and Xe. Fits of the experimental susceptibility data are made to curves from Monte Carlo simulations, and the corresponding Ginzburg numbers  $G_i$  for each measured property are deduced. Also the first correction amplitudes for the confluent singularities are obtained from the fit of the data. The respective ratios of these numbers and those obtained for the coexistence curves for  $^3\text{He}$  and Xe, presented elsewhere, are discussed in terms of predictions.

## I. INTRODUCTION

The interest in crossover phenomena from the asymptotic to mean-field critical behavior in fluids has been described in detail in a recent review article by Anisimov and Sengers [1], which lists many references and where different theoretical approaches and also a comparison with some experiments are presented. The subject of a recent paper [2] was a comparison between predictions for the crossover from Monte Carlo calculations [3] and experimental data of simple fluids. The susceptibility  $\chi^+$  above  $T_c$  (or compressibility) and the liquid and vapor densities along the coexistence curve (CXC) for Xe and  $^3\text{He}$  were studied. From a fit of the data to the predicted curves, the corresponding Ginzburg numbers  $G$  could be

---

\*To appear in: Proceedings 2000 NASA/JPL Investigators Workshop on Fundamental Physics in Microgravity. D. Strayer, Editor

estimated. For the CXC, the exit of the fluid from the critical regime into a background behavior could be clearly seen by a systematic departure from the predicted curve, well before the regime of mean-field critical behavior could be reached. For  $\chi^+$ , the behavior of Xe, a “classical fluid”, agreed well with predictions, but there were systematic differences for  ${}^3\text{He}$ , and a qualitative discussion was made in terms of the interplay between quantum and critical fluctuations for this fluid.

The purpose of this progress report is to extend the same analysis to the susceptibility  $\chi^-$  data below  $T_c$  for Xe and  ${}^3\text{He}$ , and also to give a status report on this program. After a background review, the susceptibility data of several experimental groups, namely along the critical isochore ( $T > T_c$ ) and along the liquid and the vapor side of the CXC ( $T < T_c$ ), are discussed. Comparison is made with curves from Monte Carlo calculations [3], and the corresponding Ginzburg numbers  $G(\chi^-)$  are estimated. The internal consistency for the Ginzburg numbers so obtained is checked by determining  $G$  from the fit of data to a 2-term series expansion representing part of the curve obtained from the MC calculations. From the collection of Ginzburg numbers obtained so far [ $G(\chi^+)$ ,  $G(\chi^-)$  and  $G(\text{CXC})$ ], their ratios are discussed in the light of predictions. In spite of the uncertainties in the  $G(\chi^-)$  below  $T_c$  due sparsity of data and experimental scatter, and also in the  $G(\chi^+)$  for  ${}^3\text{He}$ , some preliminary conclusions can be made. This progress report is to draw attention to the interest of such results, to their present incomplete understanding and to the great need of better data.

## II. A SHORT REVIEW

### A. Properties considered

We now list the properties discussed in this paper, and introduce the definitions of reduced temperature and density,  $t \equiv (T - T_c)/T_c$  and  $\Delta\rho \equiv (\rho - \rho_c)/\rho_c$ . The coexistence curve is expressed by

$$\Delta\rho_{LV} = (\rho_{\text{liq}} - \rho_{\text{vap}})/\rho_c = B_0(-t)^\beta[1 + B_1(-t)^{\Delta_1} + B_2(-t)^{\Delta_2} \dots] \quad (1)$$

where  $\rho_{\text{liq}}$ ,  $\rho_{\text{vap}}$  and  $\rho_c$  are the densities in the coexisting liquid and vapor phases, and at the critical point. Furthermore  $\beta = 0.326$  is the critical exponent and the bracket includes the correction-to-scaling confluent singularity terms. Here the  $B_i$ 's are amplitudes characteristic of the fluid, and  $\Delta_1 = 0.52$ ,  $\Delta_2 = 1.04$  are the exponents obtained by Wegner [4] and by Newman and Riedel [5].

The susceptibility  $\chi$  of the fluid, namely the analog of the susceptibility of a magnet, is given by  $\chi \equiv (\partial\rho/\partial\mu)_T = \rho^2\beta_T$ , where  $\beta_T$  is the isothermal compressibility and  $\mu$  is the chemical potential. As discussed by Sengers and Levert Sengers [6], the 3-D lattice-gas model (which corresponds to the 3-D Ising model in magnets) has properties that adequately describe real fluids. One particular aspect is that of symmetry in the  $\mu - \Delta\rho$  plane. (In this respect,  $^3\text{He}$  is the fluid that best conforms to this model. See Appendix) As a consequence, the derivative  $\chi$  is a symmetric function of  $\Delta\rho$  along an isotherm. Hence below  $T_c$ , one obtains  $\chi_{\text{Liq}} = \chi_{\text{Vap}}$ , where the susceptibilities are measured on both sides of the coexistence curve, and therefore we expect consistency between the data on both liquid and the vapor sides. Here we introduce the reduced quantity  $\chi^* \equiv \chi(P_c/\rho_c^2)$ , where the critical parameters have been listed in ref. [2]. Above  $T_c$  and along the critical isochore,  $\chi^* = \beta_T P_c$ .

Similarly to Eq.1, the expansion for the susceptibility  $\chi^{*(+,-)}$  from the asymptotic critical regime is given by

$$\chi^{*(+,-)} = \Gamma_0^{(+,-)}|t|^{-\gamma}[1 + \Gamma_1^{(+,-)}|t|^{\Delta_1} + \Gamma_2^{(+,-)}|t|^{\Delta_2} + \dots] \quad (2)$$

where the indices + and - indicate the region  $t > 0$  along the critical isochore and  $t < 0$  along the coexistence curve, respectively. Here again the  $\Gamma_i$ 's are amplitudes characteristic of the fluid and  $\gamma = 1.24$  is the critical exponent. The ratio  $\Gamma_0^+/\Gamma_0^-$  for a given fluid has been calculated from series expansion by Liu and Fisher to be [7]

$$\Gamma_0^+/\Gamma_0^- = 4.95 \pm 0.15 \quad (3)$$

This compares with the value of 4.82 obtained from the ratio  $(\gamma/\beta)[(1 - 2\beta)\gamma/2\beta(\gamma - 1)]^{\gamma-1}$  predicted from the parametric representation of the equation of state [8], where  $\gamma = 1.24$

and  $\beta = 0.327$  were used. The most recent values of this ratio (see [9]) are very close to 4.77. Predictions for the ratio of the amplitudes  $B_1$ ,  $\Gamma_1^+$  and  $\Gamma_1^-$  will be presented below.

## B. Ginzburg numbers and amplitude ratios

The Ginzburg criterion and Ginzburg number have been discussed in detail in the article by Anisimov, Kiselev, Sengers and Tang [10] on the crossover approach to global critical phenomena in fluids. The Ginzburg number  $G$  is seen as a dimensionless temperature, obtained from the criterion  $t \gg G$  which gives an estimate for the range of  $t$ , where the classical critical theory is valid, this is where the fluctuation contribution is small. For fluids, an order of magnitude estimate [10] of  $G$  leads to  $\approx 10^{-2}$ , and furthermore for a 3-D fluid, one finds  $G \propto R^{-6}$ , where  $R$  is the normalized molecular interaction range [10]. Hence the asymptotic critical behavior takes place for  $t \ll G$  while the classical critical behavior is expected for  $1 \gg t \gg G$ . However as pointed out in ref. [1], in ordinary fluids the crossover is never completed in the critical domain ( $t \ll 1$ ) since  $R$  is of the same order as the distance between molecules. The Monte Carlo algorithm developed by Luijten and Bloete [11] allows the full crossover region in 3-D Ising models to be covered. The calculation then gives a curve of a given singular property  $f_i = f_i(|t|/G_i)$  covering  $\approx 8$  or more decades in  $|t|/G_i$ , and is clearly more complete than the expansion series expressed in correction-to scaling terms of series. A simple check for the internal consistency in determining  $G$  can be made by the expected expansion in terms of the corrections-to-scaling confluent singularities as

$$f_i = A_{0,i}|t|^{-\lambda_i}[1 + A_{1,i}(|t|/G_i)^{\Delta_1} + \dots] \quad (4)$$

where the amplitude  $A_{0,i}$  is non-universal but where the numerical coefficients  $A_{1,i}$ , and the exponent  $\lambda_i$  are universal for all fluids and characteristic of the property (susceptibility, CXC etc...). A fit of the curves  $f_i = f_i(|t|/G_i)$ , calculated by the Monte Carlo approach [3], to Eq. 4 (restricted to the region of  $|t|/G_i$  where higher terms are negligible) gives  $A_1(\chi^+) = 0.10$ ,  $A_1(\chi^-) = 0.65$ , and  $A_1(CXC) = 0.23$ .

Of particular interest here is the calculation of the susceptibility  $\chi$ , both below and above  $T_c$ , represented in a very sensitive way by the plot [3] of the effective exponent  $\gamma_{eff}$ , which is given by the derivative

$$\gamma_{eff} \equiv -\frac{d \ln \chi_T^*}{d \ln |t|}. \quad (5)$$

In Fig.1, the plots of  $\gamma_{eff}^{(+,-)}$  versus  $|t|/G^{(+,-)}(\chi)$  for  $t > 0$  and  $t < 0$ , as obtained from Monte Carlo calculations, are presented side-by-side for comparison. The various symbols denote the successively larger values of the interaction range  $R$  that were used to generate the master curve as the distance from  $T_c$  is increased. The lines labeled “BK, BB and SF” for  $t > 0$  and “App” for  $t < 0$  are theoretical curves described in ref. [3]. The slope of the exponent,  $-\partial \gamma_{eff} / \partial \ln |t|$ , gives information on the crossover width between the asymptotic Ising value of  $\gamma = 1.24$  and the mean-field one  $\gamma = 1$ . This width is shown to be much narrower for the region  $t < 0$  than for  $t > 0$ , as was pointed out in ref. [3]. We shall see that this difference in crossover width is reflected in the data for  $^3\text{He}$ .

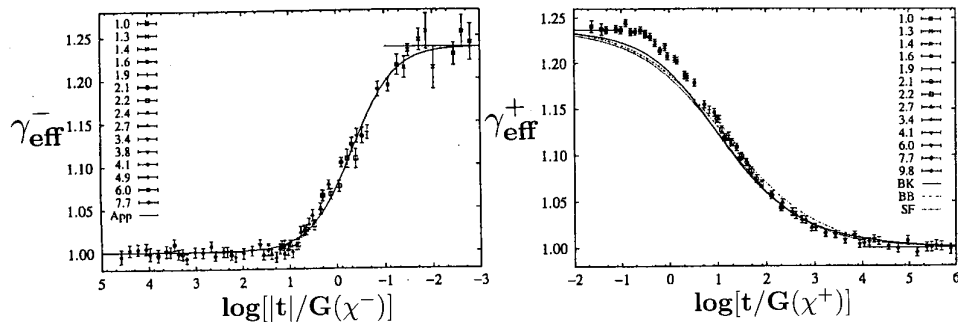


Figure 1: The effective exponents  $\gamma_{eff}^-$  for  $t < 0$  (left side) and  $\gamma_{eff}^+$  for  $t > 0$  (right side) as a function of  $|t|/G^{(+,-)}(\chi)$ . This figure has been reproduced from the paper by Luijten and Binder where the symbols (Monte Carlo calculations) and the curves (predictions “BB”, “BK” and approximation “App”) are described.

The relations between the G's and the first Wegner terms in the correction to scaling follow from Eqs. 1, 2 and 4. For instance in the case of the susceptibility above  $T_c$ , one has

$$\Gamma_1^+ = A_1(\chi^+) [G(\chi^+)]^{-\Delta_1} \quad (6)$$

with  $\Delta_1 = 0.5$ , which will be used in the discussion of the data analysis.

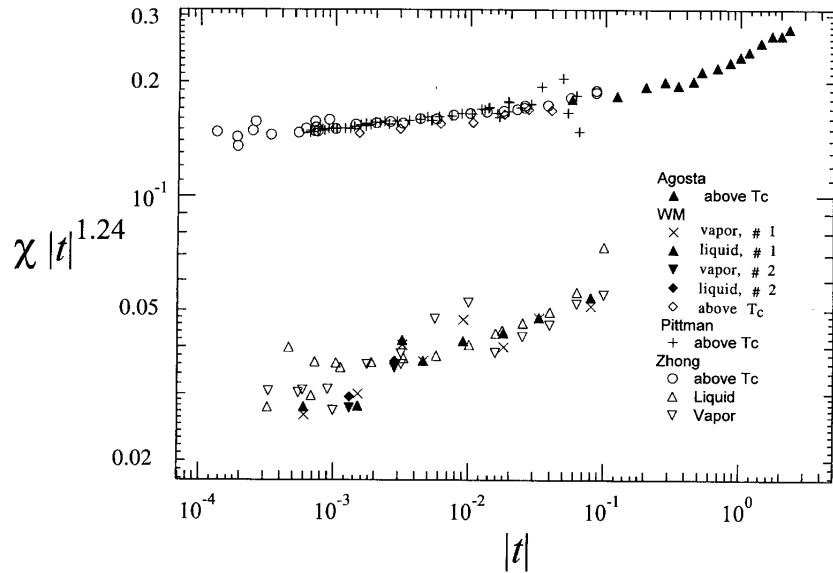


Figure 2: Experimental reduced susceptibility ( $\chi^*$ ) data for  ${}^3\text{He}$  above and below  $T_c$  (upper and lower figures) versus  $|t|$ . The references are respectively Agosta:[18]; WM:[17]; Pittman:[20]; Zhong:[19] taken at the JPL laboratory

Aharony and Ahlers [12] have discussed the ratios of the amplitudes of the “correction-to-scaling confluent singularity” terms in expressions such as Eqs. 1 and 2 for different properties, and in particular for the order parameter (here CXC) and the susceptibility above  $T_c$  versus  $|t|$ . They expressed thermodynamic quantities with singularities at the critical point as

$$f_i = A_{0,i} |t|^{-\lambda_i} [1 + a_i |t|^{\Delta_1} + O|t|^{2\Delta_1}] \quad (7)$$

where  $\lambda_i$  is the (asymptotic) critical exponent of the property  $i$ , such as susceptibility,

specific heat, order parameter etc.. and the  $a_i$ 's are the amplitudes of the first correction-to-scaling term of the confluent singularity (already introduced here as  $\Gamma_1$  and  $B_1$ ). Among the relations they derived, one which considers the ratio of the correction term amplitudes for two properties  $i$  and  $j$  of a fluid is of particular interest to us, namely

$$(\lambda_{i,eff} - \lambda_i)/(\lambda_{j,eff} - \lambda_j) = a_i/a_j \quad (8)$$

Here  $\lambda_{i,eff}$  is the effective exponent and  $\lambda_{i \text{ or } j}$  is the asymptotic exponent with  $\lambda_i = \gamma = 1.24$  and  $-\lambda_j = \beta = 0.326$ . The numerical values for  $\lambda_{i,eff}$  are obtained by fitting experimental data to a simple power law over the same range of  $|t|$  where the fit to Eq. 7 has been made. A prediction of the ratio of Ginzburg numbers via Eqs.4 and 7 can therefore be made and compared with that from experiments. One has

$$(G_j/G_i) = [a_i A_1(j)/a_j A_1(i)]^{1/\Delta_1}. \quad (9)$$

Here  $A_1(j)/A_1(i)$  is the ratio of the numerical coefficients in Eq.4 for the properties  $j$  and  $i$ , listed after Eq.4.

Bagnuls, Bervillier, Meiron and Nickel [13] have calculated the ratios  $a_i/a_j$  using “massive field theory” for the  $\Phi^4$  model in 3-D for the  $n=1$  class. These ratios are universal and are found to be  $a(\chi^+)/a(\chi^-) = \Gamma_1^+/\Gamma_1^- = 0.315 \pm 0.013$  and  $a(\chi^+)/a(CXC) = \Gamma^+/B_1 = 0.9 \pm 0.2$ . (See Tables VIII and IX of ref [13]). This implies that the ratio of the Ginzburg numbers is universal too. From Eq.9 one then obtains  $G(\chi^+)/G(\chi^-) = 0.23 \pm 0.01$  and  $G(\chi^+)/G(CXC) = 0.15 \pm 0.07$ .

### III. EXPERIMENTAL DATA AND DETERMINATION OF $T_C$

In the experiments,  $\chi$  has been determined either from the intensity of light scattering (Xe) [14,15] or from the measurements of the density versus pressure along isotherms in Xe [16], and in  $^3\text{He}$  [17,21,18,19] and from the vertical density gradient in the gravity field for  $^3\text{He}$  [20] above  $T_c$ . Here we briefly comment on the various measurements and their respective scatter.

As will be seen below, the  $\chi$  data for  $t > 0$  have an appreciably higher accuracy than those below  $T_c$ . In the light scattering measurements, this might possibly be due to the added difficulty of sending the laser beam alternatively into the superposed liquid and vapor phases of a cell with a small height, and where the meniscus will become concave as  $T_c$  is approached, because of the decreasing surface tension. This contrasts with measurements above  $T_c$  where the beam is positioned near mid-height of the cell, and where the maximum light scattering intensity is observed by slowly scanning the vertical position. In the present analysis, the data by Smith et al [15] above  $T_c$  have not been used, because their scatter is larger than that of the more recent data by Güttinger and Cannell [14]. However we note that in ref [15] the amplitude ratio is  $\Gamma_0^+/\Gamma_0^- = 4.1$ , which is not far from the predictions. If the data of ref [14] above  $T_c$  are combined with those below  $T_c$  [15], a ratio of  $5.8 \pm 0.4$  is obtained by fitting both sets of data to Eq. 2. The amplitudes are listed in Table I.

The maximum value of  $\chi^+$  at  $\rho_c$  from isotherm data above  $T_c$  is obtained with a higher precision than is the extrapolation of  $\chi^-$  to the coexistence curve below  $T_c$ . As mentioned above, it is expected from the Ising model that  $\chi_{vap} = \chi_{liq}$ . Yet there can be appreciable scatter in both determinations which reflects the uncertainties both in the differentiations of the  $\rho(P)$  data sets and also in the factor  $\rho_{Vap}^2$ , or  $\rho_{Liq}^2$ . The results are presented as reduced quantities  $\chi^* \equiv \chi P_c / \rho_c^2$ , where the critical parameters have been listed in ref. [2]

In the experiments with Xe where optical methods were used, the determination of the critical temperature has been achieved for the  $\chi$  measurements by observing the disappearance of the meniscus, and by a fit to Eq.2 [14]. The coexistence curve data were fitted to Eq.1 [22]. On the average these determinations were made with an uncertainty of  $\delta t \approx \pm 5 \times 10^{-6}$ .

By contrast in the experiments with  ${}^3\text{He}$  without optical access, the uncertainty in  $T_c$  is more important. It is probably smallest in the experiments by Pittman *et al.* [20] where  $T_c$  was determined principally from measurements below  $T_c$  (coexistence curve), and where  $T_c$  was obtained from a fit of Eq.1, as described in that paper. Here the claimed uncertainty is  $\delta T_c/T_c \approx \pm 9 \times 10^{-6}$ . In the older measurements of  $\chi$  from isotherms by Wallace and Meyer [17], the choice of  $T_c$  was obtained by extrapolation of both coexistence curve data

and compressibility data, and based on a simple power law with effective exponents. The uncertainty was claimed to be  $\delta T_c/T_c \approx \pm 6 \times 10^{-5}$ . The use of this power law led to a systematic error in  $T_c$  which was evidenced by deviations from the compressibility data of ref. [20], as shown in Fig.1 of [20]. In the  $\chi$  measurements by Chase and Zimmerman [21], also from isotherms, the determination of  $T_c$  was done in a similar way as in ref [17]. In the most recent measurements of  $\chi$  from isotherms by the MISTE team at JPL [19], the value of  $T_c$  was determined from a fit of the  $\chi$  data above  $T_c$  to Eq. 6 with a systematic uncertainty of  $\delta T_c/T_c \approx \pm 1.5 \times 10^{-5}$  in  $T_c$  (F. Zhong, private communication).

#### IV. DATA PRESENTATION AND MONTE CARLO CALCULATIONS

In Fig.2 the susceptibility data for  ${}^3\text{He}$  from refs [17,20,19,18] are presented, both above and below  $T_c$ , scaled by the leading singularity  $|t|^{-\gamma}$ . The data of ref [21] lie systematically up to 20% below the other data sets and have not been included in the plot to avoid overcrowding the figure. The data of ref [20] can be made to agree well with those of ref. [19], if their respective values of  $T_c$  are slightly shifted well within the stated uncertainty mentioned above. The shifts are as follows:  $\delta T_c/T_c = +6 \times 10^{-6}$  for data of ref. [19] and  $\delta T_c/T_c = -6 \times 10^{-6}$  for data of ref. [20]. By combining the two sets of data with the mutually shifted  $T_c$ , a fit to Eq. 2 gives  $\Gamma_0^+ = 0.145$ . For a given set of experiments, where data above and below  $T_c$  were obtained, the same choice of  $T_c$  was implemented. The error in  $T_c$  in the experiments of ref [17] was corrected by an appropriate shift  $\delta T_c$  within the stated uncertainty, which resulted in the data above  $T_c$  to lie uniformly  $\approx 5\%$  below those of refs. [20] and [19].

Table I lists the amplitudes of the leading terms  $\Gamma_0^+$ ,  $\Gamma_0^-$  and  $B_0$ , and of the first correction terms  $\Gamma_1^+$ ,  $\Gamma_1^-$  and  $B_1$  obtained by a fit of the data to Eq.1 resp. Eq. 2. The errors listed are all systematic, not statistical. The corresponding sources of data are listed in the last column. The data fits for  $\Gamma_1^+$  and  $\Gamma_1^-$  in  ${}^3\text{He}$  and for  $\Gamma_1^-$  in  $\text{Xe}$  (with very scant data and appreciable scatter close to  $T_c$ ) were made by setting the higher terms in Eq. 1 to zero. To

for this purpose, the fitting was restricted to the range  $|t| < 2 \times 10^{-2}$ , where presumably the higher terms in Eqs. 1, 2 (and therefore also in Eq. 4) can be neglected. Because of the strong correlation between the amplitudes in the data fitting procedure to Eqs 1 and 2, an uncertainty of only say  $O(\pm 5\%)$  in  $\Gamma_0$  can produce a much larger one of  $O(\pm 50\%)$  in  $\Gamma_1$ . For the CXC of  $^3\text{He}$  and Xe, and for  $\Gamma_1^+$  of Xe, the amplitudes listed in refs [14,20,22] were used.

The  $^3\text{He}$  data by Pittman *et al.*, which result from measuring the density difference between two superposed sensors, show a smaller scatter close to  $T_c$  than those ref. [19], but they are restricted to the range  $t > 5 \times 10^{-4}$ , below which the vertical density profile becomes sharply non-linear as stratification from gravity increases. Above  $t > 5 \times 10^{-2}$ , where  $\chi$  has become small, this method is no longer sensitive, as shown by the rapidly increasing scatter. One notes that for the  $^3\text{He}$   $\chi^-$  data, the leading amplitude  $\Gamma_0^-$  is consistent well within the large scatter with the expected  $\Gamma_0^- = \Gamma_0^+ / 4.95 = 0.029$  where the factor 4.95 was given in Eq. 3. Here we have taken  $\Gamma_0^+ = 0.145$ , the value from the combined set of data from refs. [20] and [19]. In spite of the data scatter below  $T_c$ , the difference in the change of  $\chi |t|^{1.24}$  with  $|t|$  in the regime above and below  $T_c$  is quite striking :  $\mathcal{R}(t=0.1)/\mathcal{R}(t \rightarrow 0) = 1.25$  compared to  $\mathcal{R}(-t=0.1)/\mathcal{R}(t \rightarrow 0) = 1.93$ , where  $\mathcal{R}(t) \equiv \chi |t|^{1.24}$ . This is consistent with the finding that  $\gamma_{eff}(t < 0)$  is smaller than  $\gamma_{eff}(t > 0)$  over the common experimental range  $10^{-3} < |t| < 10^{-1}$ . As was mentioned before, MC calculations predict that the crossover width is narrower for  $t < 0$  than for  $t > 0$ .

In Figs. 3 and 4, plots of the scaled reduced and normalized susceptibility  $\bar{\chi} |t|^{1.24}$  versus  $|t|/G(\chi^{(+,-)})$  are shown. Here  $\bar{\chi} = \chi^*/\Gamma_0^{(+,-)}$ , as in ref. [2]. In each figure the subscripts indicate the phase (vapor or liquid) along the coexistence curve. In the limit  $|t| \rightarrow 0$  the ratio  $\bar{\chi} |t|^\gamma$  becomes unity. However the MC calculations for  $t < 0$  have more scatter than for  $t > 0$  as seen from Fig.1. In spite of this, their trajectory for  $[(-t/G) < 1 \times 10^{-2}]$  can be estimated quite well, since with decreasing  $|t|$  the curves will follow Eq.4, and tend to unity. The values of the  $\Gamma$ 's and  $G(\chi^+)$  obtained via Eq. 6 and similarly of  $G(\chi^-)$  and  $G(CXC)$  for both fluids are shown in Table 1.

In Fig.3 both the susceptibilities [14,16,15] above and below  $T_c$  for Xe are presented, - the first one already shown in ref [2]. Below  $T_c$ , there are few data points, and the scatter prevents a precise determination of  $\Gamma_0^-$  and therefore the resulting value of  $G(\chi^-)$  is much more uncertain than that of  $G(\chi^+)$ . It should be mentioned, as was done in ref. [2], that the fit for  $t > 0$  was made taking  $\Gamma_0 = 0.0594$  instead of 0.0577 obtained in ref. [14]. This choice of  $\Gamma_0$ , determined by the adopted value of  $\gamma = 1.240$ , is no doubt responsible for the different values of  $G(\chi^+)$  obtained from the data fit to Eq.2 and to the MC curve, respectively 0.006 and 0.018, as reported in ref [2].

Fig.4 shows the plots for  ${}^3\text{He}$  of refs [20,19,17,18] of Fig.2, with  $\Gamma_0^+ = 0.145$ . For  $\chi^-$ , the value  $\Gamma_0^- = 0.029$  mentioned above was used, which “anchors” the data presentation  $\bar{\chi} t^{1.24}$  in the asymptotic regime. The fit according to Eq.2 is restricted to  $|t| < 3 \times 10^{-2}$ . The top plot is different from that of ref [2] as it combines the data of refs [19] and [20] as has been described above. The new value of  $\Gamma_0^+ = 0.145$  (instead of 0.139) then leads to a larger value of  $G(\chi^+)$ , listed in Table 2. [By accident, in the bottom plot for  $t < 0$ , the symbols WM(vapor) and JPL (liquid) on one hand, and WM(liquid) and JPL(vapor) on the other, are undistinguishable]. It is clear that the restricted data range in  $|t|/G(\chi^-)$  for  ${}^3\text{He}$  below  $T_c$  does not enable confirming the variation of the quantum fluctuations in the crossover region, proposed for  $t > 0$  [2], where the data extend beyond  $t = 10^{-1}$ .

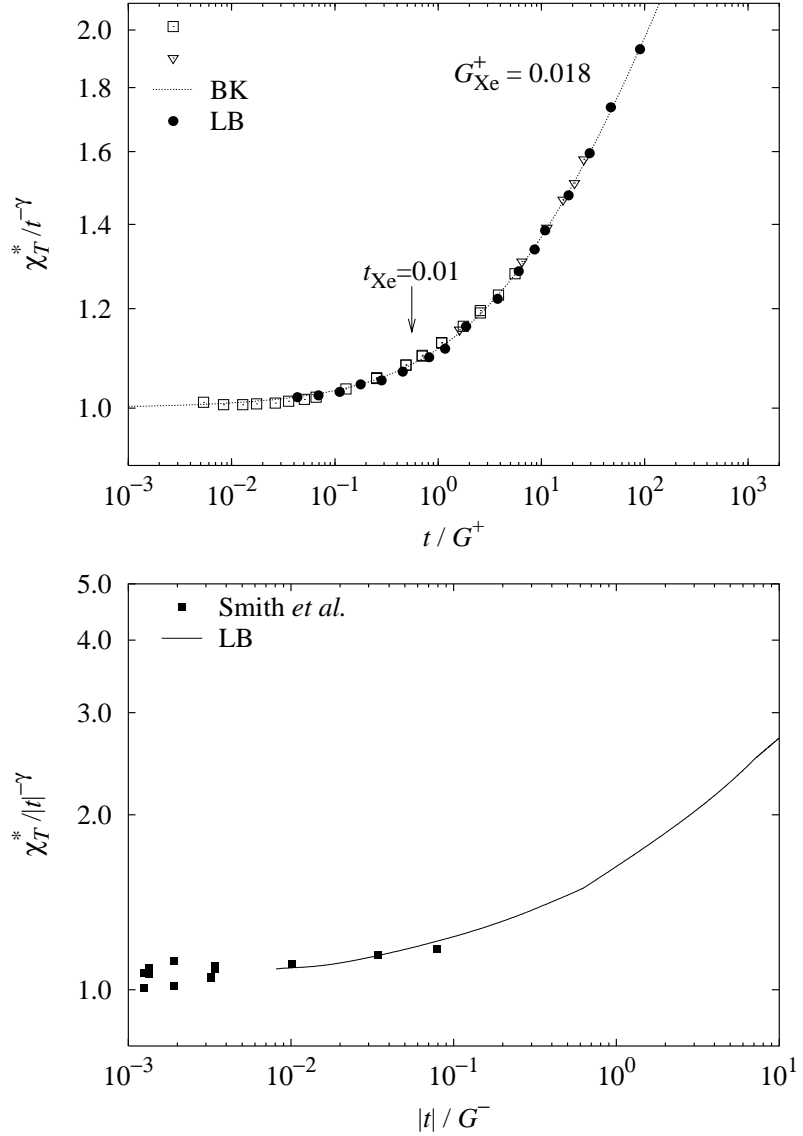


Figure 3: Experimental susceptibility data for Xe above and below  $T_c$  (upper and lower figures) versus  $|t|/G(\chi^{(+,-)})$ , fitted to the Monte Carlo calculations (solid circles LB and lines LB). Dotted line: Renormalization Group (BK) for Belyakov and Kiselev, referred to in [3]. Experimental data: open squares: [14], open inverted triangles:[16], solid squares:[15]. Here the  $\chi^*$ 's have been divided respectively by  $\Gamma_0^+$  and  $\Gamma_0^-$

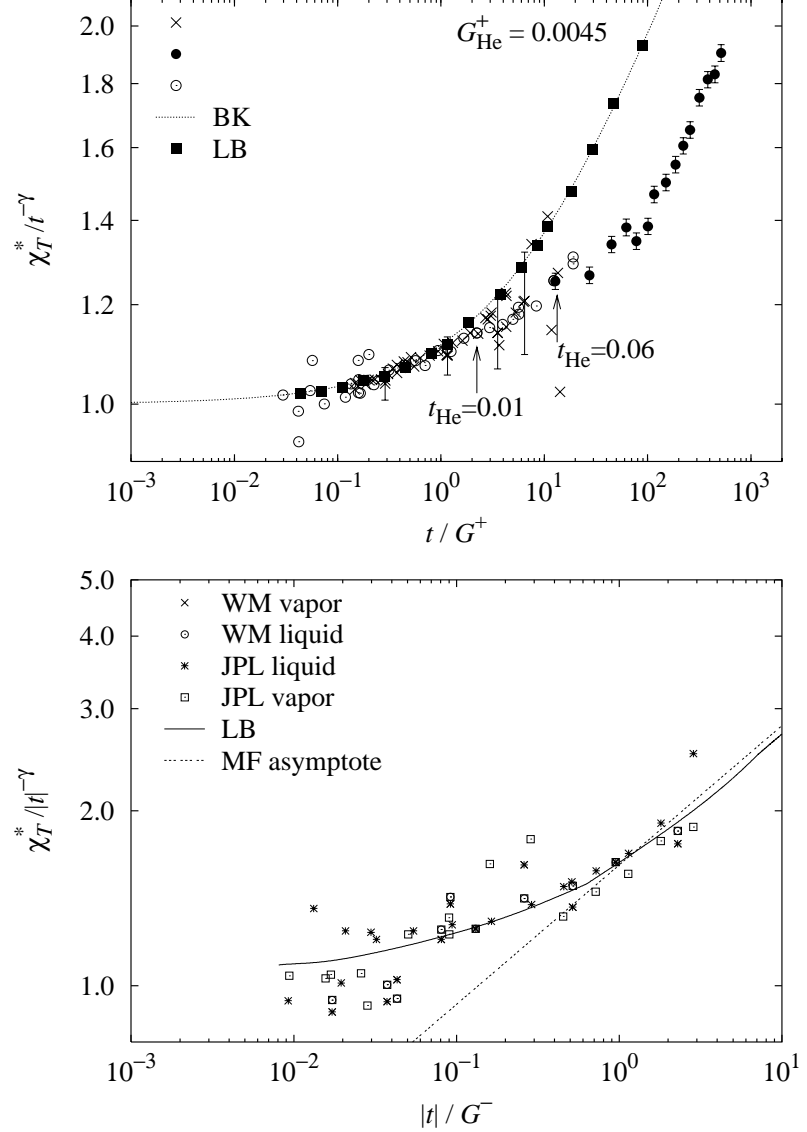


Figure 4: Experimental susceptibility data for  ${}^3\text{He}$  above and below  $T_c$  from fig.2, (upper and lower figures) versus  $|t|/G(\chi^{(+,-)})$ , fitted to the Monte Carlo calculations (solid squares (LB) ( $t > 0$ ) and solid line ( $t < 0$ ). Dotted line: Renormalization Group (BK), as described in [3]. Dotted line labeled MF: Mean Field asymptote. Experimental data for  $t > 0$ : X:[20]; solid circles:[18]; open circles [19]. For  $t < 0$  : WM :[17]; JPL: [19]. Here the  $\chi^*$ 's have been divided respectively by  $\Gamma_0^+$  and  $\Gamma_0^-$

## V. DISCUSSION

In Table 1, the values of the first correction term amplitudes, obtained from a fit of the experimental data to Eqs.1 and 2 are obtained and their ratios are compared with predictions [13]. The large (systematic) error bars reflect the data scatter and fit quality. A fair consistency within the large uncertainties is obtained, indicating that the result from the data analysis appears consistent with the universality prediction based on the  $\Phi^4$  model.

In Tables 1 and 2, the Ginzburg numbers and relevant ratios are listed, and the results are now briefly discussed. Here again the error bars are guesses based on the fitting uncertainties, since a satisfactory error calculation could not be done. In Table 2, the G's are those obtained by a fit of the data to the curve obtained from Monte Carlo calculations. Obviously one of the great merits of MC calculations is to give a much wider range of  $|t|/G$  where the data can be fit to predictions than can a 2-term expansion such as Eqs 1 and 2. At the same time, it is instructive to compare the resulting G's obtained from both methods.

Fluid	$\Gamma_0$	$\Gamma_1$	$B_0$	$B_1$	$G()$ from $\Gamma_1^{(+-)}$ , $B_1$	Refs.
Xe	[+] 0.0577	[+] $1.29 \pm 0.2$	-	-	$(\chi^+)$ 0.006	Guettinger&Cannell
	[+] 0.013	[+] $1.4 \pm 0.5$			$(\chi^-)$ 0.2	Smith et al.*
${}^3\text{He}$	[+] 0.141	[+] $1.5 \pm 0.2$	1.47	1.17	(CXC) 0.035	Naerger&Balzarini
	[+] 0.150	[+] 0.98			$(\chi^+)$ 0.0044	Pittman et al.*
	[+] 0.145	[+] $1.3 \pm 0.2$			$(\chi^+)$ 0.010	JPL,(Barmatz et al.*)
	[+] 0.029	[+] $3.6 \pm 0.3$			$(\chi^+)$ 0.006	JPL/Pittman*
					$(\chi^-)$ 0.034	JPL/Wallace *
					(CXC) $0.06 \pm 0.02$	Pittman et al.
	$\Gamma_1^+/\Gamma_1^-$	$\Gamma_1^+/B_1$				
Xe	$0.9 \pm 0.4$	$1.1 \pm 0.3$				Same refs. as above
${}^3\text{He}$	$0.36 \pm 0.07$	$1.4 \pm 0.3$				JPL/Wallace/Pittman
Theory	$0.315 \pm 0.013$	$1.1 \pm 0.2$				Bagnuls et al.

Table 1: Amplitudes for the expansions in Eqs 1 and 2 for  $\chi^+$ ,  $\chi^-$  and CXC, as obtained from fits in various experiments, and the corresponding Ginzburg numbers deduced from the amplitudes  $a_i$  in Eq.6 and similar. The symbol “\*” indicates that the expansion was limited to the first correction term and to  $|t| < 10^{-2}$ . The bottom three rows show the comparison between the experimental and the predicted (universal) ratios of the first correction amplitudes. For  ${}^3\text{He}$ ,  $\Gamma_1^+ = 1.3$  was used.

Fluid	$G(\chi^+) \times 10^2$	$G(\chi^-) \times 10^2$	$G(CXC) \times 10^2$	$G(\chi^+)/G(\chi^-)$	$ G(\chi^+)/G(CXC) $
Xe	$1.8 \pm 0.3$	$10 \pm 5$	$7 \pm 2$	$0.18 \pm 0.08$	$0.26 \pm 0.06$
$^3\text{He}$	$0.25 \pm 0.15$ *	$3.5 \pm 2$	$7 \pm 2$	$0.07 \pm 0.04$	$0.036 \pm 0.02$
	$0.45 \pm 0.2$ **			$0.13 \pm 0.05$	$0.064 \pm 0.03$
Eqs.8 and 9 Bagnuls et al. with Eq. 9				$0.02 \rightarrow 0.2$ $0.23 \pm 0.01$	$0.10 \pm 0.02$ $0.15 \pm 0.07$

Table 2: The Ginzburg numbers, as obtained from fits of the data to Monte Carlo calculations, and their ratios, with estimated uncertainties, and comparison with predictions via Eq. 8 of ref[12] and Eq. 9. Notation indices: “ \* ” obtained with Pittman data and  $\Gamma_0^+ = 0.140$ . “ \*\* ” obtained with combined Pittman/JPL data and  $\Gamma_0^+ = 0.145$ . The numerical values in the bottom row are those predicted in Ref.[13] with use of Eq.9.

This is done by comparing the numbers in the last column of Table 1 with those on the first three columns in Table 2. On the whole, there is acceptable consistency between the determination from both methods, with the exception for Xe. This might be caused by the different choices of  $\Gamma_0$  for the the  $\chi^+$  data, as mentioned before.

We note that the Ginzburg numbers have uncertainties that reflect the degree of difficulty in fitting the data to the curve obtained from Monte Carlo calculations. Yet, even with this caveat, certain tentative conclusions can be reached. First, the order of magnitude of the  $G_i$  is as expected [1], namely  $O(10^{-2})$ . Second, the ratios  $G(\chi^+)/G(\chi^-)$  are roughly the same for Xe and  $^3\text{He}$ , within the stated uncertainty. From [12] it is not clear whether there should be universality for this ratio or for  $G(\chi^+)/G(CXC)$ , where the experimental values for both fluids are different. But as noted before, universality for the ratios of the first correction term amplitudes is predicted from the  $\Phi^4$  model [13], and therefore the ratios of the corresponding Ginzburg numbers, obtained via Eq.9, are universal too.

We now compare the ratios with those expected, based on ref [12]. For  $^3\text{He}$ , the measured effective exponents for  $\chi$  were  $\gamma_{eff}^+ = 1.19$  [17,21,20] and  $\gamma_{eff}^- = 1.08$  [17,21] over the range  $5 \times 10^{-4} < |t| < 5 \times 10^{-2}$ . When these  $\chi$  data were published, this result was very

surprising, because it was expected that the exponents should be the same both above and below  $T_c$ . However in the light of the Monte Carlo calculations that show the crossover to be quite different on both sides of  $T_c$  (See Fig.1), this discrepancy in the values of  $\gamma_{eff}$  can be understood. Interestingly the susceptibility data for Xe [15] do not show this difference, and both effective exponents are listed [15] as  $\gamma_{eff}^{(+,-)} = 1.21$  over the range  $2 \times 10^{-4} < |t| < 8 \times 10^{-3}$ . For the coexistence curve, the effective exponent has been reported to be  $\beta_{eff} = 0.360$  for  ${}^3\text{He}$  [17,21,20] and 0.355 for Xe [23].

The predicted ratios  $G(\chi^+)/G(CXC)$  and  $G(\chi^+)/G(\chi^-)$  from Eqs.8 and 9, and from Bagnuls et al. [13] via Eq.9 are listed in Table II. Starting with the results from ref. [12],  $G(\chi^+)/G(CXC) \approx 0.10$  is determined from the effective exponents and lies in between the values listed for Xe and  ${}^3\text{He}$ . This prediction, which is consistent with the value obtained by Bagnuls et al., is then good to within say  $\pm 20\%$ . There is agreement within the combined uncertainties for  ${}^3\text{He}$ , but not so for Xe. The prediction of the ratio  $G(\chi^+)/G(\chi^-)$  from ref. [12] with Eq.8, is uncertain : if  $\gamma_{eff}^+ = \gamma_{eff}^-$  is taken, as appears to be the case for the Xe data, the ratio is 0.2. However when the values for  $\gamma_{eff}^+$  and  $\gamma_{eff}^-$  for  ${}^3\text{He}$  are used, as listed above, the ratio becomes 0.02 ! The first value is consistent with the predictions by Bagnuls et al.. Overall the experimental data analysis in terms of the correction term amplitudes  $a_i$  and the  $G_i$ 's is still in a preliminary state and further progress is needed.

## VI. CONCLUSION

A status report has been presented of the program describing the crossover from asymptotic to mean-field behavior in different properties for two simple fluids. So far, our understanding is incomplete, since the accuracy of several sets of experimental data needs substantial improvement. By contrast, MC calculations [3] are making precise predictions of the crossover for the susceptibility  $\chi^+$  and  $\chi^-$  as well as the coexistence curve in terms of Ginzburg numbers. Also there are quantitative predictions of the ratios of the correction term amplitudes [13].

In spite of the uncertainty in experimental data, some conclusions can be reached. The Ginzburg numbers for  $\chi$  and CXC in  ${}^3\text{He}$  and Xe and their ratios have been obtained from a data analysis. The latter were compared with predictions and discussed. Also from the ratios of the first correction term amplitudes  $B_1$ ,  $\Gamma_1(\chi^+)$  and  $\Gamma_1(\chi^-)$ , there appears confirming evidence of their predicted universality within the large uncertainties. Further progress can be expected when better experimental data of the susceptibility of Xe and  ${}^3\text{He}$  below  $T_c$ , and over a larger temperature range have been obtained.

## VII. ACKNOWLEDGMENTS

This research was supported by NASA grant NAG 3-1838. The greatest debt of gratitude goes to E. Luijten for the very stimulating and informative interactions with him and for his generous effort in preparing several plots. Furthermore he made a detailed criticism of this paper. I am also indebted to A. B. Kogan for his help with the plots in Fig.2, with data fitting and for his technical help with the formatting, to G.O Zimmerman for supplying an original figure of the Chase and Zimmerman  $\chi$  data, to M. Barmatz and F. Zhong for permission to use the unpublished  $\chi$  data (labeled Zhong and JPL in the figures) obtained in the JPL MISTE project, and to M. Giglio for supplying tabulations of  $\chi^-$  in Xe. I am very grateful to J.M.H. Levelt Sengers for correspondence on the V.d.W. model and to F. Zhong for comments on this report and for very useful suggestions. Finally I am indebted to C. Bervillier for correcting some references, and to him and to E. Vicari and A. Pelissetto for bringing those in [9] to my attention.

## VIII. APPENDIX

### A. Extension of the rectilinear diameter above $T_c$ ?

In the course of the data analysis for obtaining the  $\chi^+$  of Xe from ref. [16], the location of the maximum for  $\chi^+$  with respect to the critical isochore was determined. This line of

points might be thought to extend the trajectory of the rectilinear diameter as  $T$  increases and passes the critical point. Over the whole range of the data ( $t < 0.47$ ) it was found to have a slope  $\Delta\rho/t = -0.049$ , to be compared with the slope of  $-0.725$  for the rectilinear diameter [23]. In the Ising model, the slope is zero for both lines. Similarly the Van der Waals model predicts the rectilinear diameter slope as  $-2/5$  [6], and from an expansion above  $T_c$  the slope for the maximum of  $\chi^+$  to be zero [24]. Hence there is a slope discontinuity in the same direction as observed in Xe. For  ${}^3\text{He}$ , experiments give a rectilinear diameter slope of  $+0.022$  [20]. Above  $T_c$  from an inspection of the the maximum location in  $\chi^+$  in the data analysis of various experiments [25], the slope is found to be zero within experimental error over the range  $t < 2 \times 10^{-1}$ . Beyond this range, the  $\chi^+$  versus  $\rho$  curve along an isotherm is no longer symmetric with respect to  $\rho_c$  and as  $t$  increases, the maximum of  $\chi^+$  shifts to larger densities.

---

- [1] M.A. Anisimov and J.V. Sengers " Critical and Crossover Phenomena in Fluids and Fluid Mixtures" To appear in "Supercritical Fluids-Fundamentals and Applications" E. Kiran, P.G. Debenedetti and C.J. Peters, Eds, (Kluwer, Dordrecht).
- [2] E. Luijten and H. Meyer, Phys. Rev. E **62** 3257 (2000).
- [3] E. Luijten and K. Binder, Phys. Rev. E **58** 4060(R) (1998).**59** 7254(E) (1999).
- [4] F. Wegner, Phys. Rev. B **5** 4529 (1972).
- [5] K.E. Newman and E.K. Riedel, Phys. Rev. B **30** 6615 (1984).
- [6] J.V. Sengers and J.M.H. Levelt Sengers, "Critical Phenomena in Classical Fluids", in Progress in Liquid Physics, C.A. Croxton, ed. (Wiley, Chichester, UK, 1978) p. 103.
- [7] A. Liu and M.E. Fisher, Physica A **156** (35) 1989.
- [8] P. Schofield, J.D. Litster and J.T. Ho, Phys. Rev. Lett. **23**, 1098 (1969).

- [9] Further values for the ratio  $\Gamma_0^+/\Gamma_0^-$  are  $4.77\pm0.3$  by C. Bagnuls et al. (ref.13);  $4.75\pm0.03$  by M. Caselle and M. Hasenbusch, J. Phys. **A** **30**, 4963 (1997);  $4.73\pm0.16$  and  $4.79\pm0.1$  by R. Guida and J. Zinn-Justin, J. Phys. **A31**, 8103 (1998),  $4.77\pm0.02$  by M. Campostrini, A. Pelissetto, P. Rossi and E. Vicari, Phys. Rev. **E** **60** 3526 (1999) and  $4.762\pm0.008$  by P. Butera and M. Comi, Phys. Rev. **B** **62** 14837 (2000).
- [10] M.A. Anisimov, S.B. Kiselev, J.V. Sengers and S. Tang, Physica A, 188, 487 (1992).
- [11] E. Luijten and H.W.J. Bloete, Int. J. Mod. Phys. **C6** 359 (1995).
- [12] A. Aharony and G. Ahlers, Phys. Rev. Lett. **44**, 782 (1980).
- [13] C. Bagnuls, C. Bervillier, D.I. Meiron and B.G. Nickel, Phys. Rev. **B** **35** 3585 (1987).
- [14] H. Güttinger and D.S. Cannell, Phys. Rev. **B** **24** 3188 (1981).
- [15] I.W. Smith, M. Giglio and G.B. Benedek, Phys. Rev. Lett. **27**, 1556 (1971).
- [16] A. Michels, T. Wassenaar and P. Louwerse, Physics **20** 99 (1954).
- [17] B.A. Wallace and H. Meyer, Phys. Rev. **A** **2** 1536 (1970). A tabulation of the susceptibility data is given in a technical report, Duke University (1972), unpublished.
- [18] C.C. Agosta, S. Wang, L.H. Cohen and H. Meyer, J. Low Temp. Phys. **67**, 237 (1987).
- [19] M. Barmatz, I. Hahn and F. Zhong, Proceedings of the 2000 NASA/JPL Investigators Workshop on Fundamental Physics in Microgravity, edited by D. Strayer, Solvang, CA, June 2000.
- [20] C. Pittman, T. Doiron and H. Meyer, Phys. Rev. **B** **20** 3678 (1979) The fit of the  $\chi^+$  data was done to a series with two correction terms in Eq.2, namely leading to  $\Gamma_0^+ = 0.139$ ,  $\Gamma_1^+ = 3.2\pm1$  and  $\Gamma_2^+ = -12\pm14$  (Their Table III). However in this fit the second term is very important, and through the strong correlation in the least squares fit, this term impacts on the value of  $\Gamma_0^+$ . Above the fit range of  $t = 2\times10^{-2}$ , the agreement with the data deteriorates very sharply. A fit with only the first term, more reasonable, gives  $\Gamma_0^+ = 0.141$  and  $\Gamma_1^+ = 1.5\pm0.2$  over the same range of  $t$ .

- [21] C.E.Chase and G.O. Zimmerman, J. Low Temp. Phys. **24**,315 (1976)
- [22] U. Naerger and D. Balzarini Phys. Rev. B **42** 6651 (1990)
- [23] A.B. Cornfeld and H.Y Carr, Phys. Rev. Lett. **29**, 28 (1972).
- [24] J.M.H. Levelt Sengers, Industrial and Engineering Fundamentals **9**, 470 (1970)
- [25] From an unpublished analysis of  $\rho$  versus  $P$  data along isotherms from Agosta et al.(ref. 16)